Available online at www.sciencedirect.com
ScienceDirect
Polymer 48 (2007) 3555–3564
polymer
www.elsevier.com/locate/polymer

Intercalated structure of polypropylene/*in situ* polymerization-modified talc composites *via* melt compounding

Xing-Ping Zhou [a], Xiao-Lin Xie [a,b,*], Zhong-Zhen Yu [c], Yiu-Wing Mai [c]

[a] *Department of Chemistry and Chemical Engineering, Huazhong University of Science and Technology, Wuhan 430074, China*
[b] *State Key Laboratory of Plastic Forming Simulation and Die & Mould Technology, Huazhong University of Science and Technology, Wuhan 430074, China*
[c] *Center for Advanced Materials Technology (CAMT), School of Aerospace, Mechanical and Mechatronic Engineering J07, The University of Sydney, Sydney, NSW 2006, Australia*

Received 31 October 2006; received in revised form 25 March 2007; accepted 19 April 2007
Available online 24 April 2007

Abstract

Talc was modified with methyl methacrylate (MMA) or butyl acrylate (BA) *via in situ* polymerization. The talc/isotactic polypropylene (PP) composites with nano-sized intercalated structure were formed by melt compounding of PP with the modified talc. The results showed that the talc layers were partially delaminated, aligned along the flow direction, and uniformly dispersed in the PP matrix. The thickness of the PMMA-modified talc layers in the PP matrix was in the range 80–240 nm, while the PBA-modified talc was even thinner. PMMA or PBA macromolecules attached on the surface of talc layers hindered the crystallization of the PP component. Moreover, the aligned pristine talc layers promoted the orientation of the PP crystals. However, the extent of PP crystal orientation decreased in the presence of PMMA or PBA-modified talc.

Keywords: Intercalation; *In situ* polymerization; Talc

1. Introduction

Polymer matrix nanocomposites have attracted considerable attention owing to their unique mechanical, optical, electric and magnetic properties resulting from the extremely large interface area between the filler and the matrix [1–4]. It is well-known that the mechanical properties of composites are strongly related to the aspect ratio and orientation of the filler. Layered silicate, such as clay, has been extensively studied in recent years due to its fairly large aspect ratio [5–8]. The layer structure of clay consists of two silica tetrahedral sheets fused to one alumina octahedral sheet. The layer thickness is around 1 nm, while its lateral dimension may vary from 50 nm to several microns. These layers organize themselves to form stacks with a regular van der Waals gap between them called the interlayer or gallery [9,10]. Isomorphic substitution within the layers (for example, Al^{3+} replaced by Mg^{2+} or by Fe^{2+}) generates negative charges that are counterbalanced by alkali or alkaline earth cations located in the interlayer. The galleries are normally occupied by cations such as Na^{+}, Ca^{2+}, and Mg^{2+}. When clay is modified with organic quaternary amine salts, such as cetyl trimethyl ammonium bromide, there will be an ion exchange between long-chain alkyl amine ions and alkali or alkaline earth cations. This leads to enlarged galleries of clay. During *in situ* intercalative polymerization or melt compounding, the monomers or polymer chains enter easily into the galleries of clay, and intercalated or exfoliated polymer/clay nanocomposites are formed [10–12].

Talc is also a tri-octahedral 2:1 layer silicate mineral, characterized by three octahedral Mg positions per four tetrahedral Si positions [13]. The resistance to heat, electricity, acids and the platy nature of talc make it an ideal reinforcement for plastics in many applications [14]. Composites filled with platy

* Corresponding author. Department of Chemistry and Chemical Engineering, Huazhong University of Science and Technology, Wuhan 430074, China. Tel.: +86 27 8754 0053; fax: +86 27 8754 3632.
E-mail address: xlxie@mail.hust.edu.cn (X.-L. Xie).

0032-3861/$ - see front matter © 2007 Published by Elsevier Ltd.
doi:10.1016/j.polymer.2007.04.033

talc always exhibit higher stiffness and creep resistance both at ambient and elevated temperatures when compared with composites filled with particulate fillers, such as calcium carbonate. It has been widely used in polymer composites to improve their thermal stability and mechanical properties, or lower their cost [15–18]. However, talc differs from clay by a unit cell layer charge (0.0 per O_{20} unit), whilst the layer charge of smectite clay, such as montmorillonite (MMT), is in the range from −0.6 to −1.4 per O_{20} unit [8]. Hence, there are no interlayer alkali and alkaline earth metal cations in its galleries [19]. Thus, talc is difficult to be intercalated with long-chain organic compounds by ion exchange. However, its zero layer charge and lack of any interlayer covalent species are responsible for the weak interlayer interaction that is limited to van der Waals attraction. Talc may have numerous crystallographic stacking faults and actual separation between sheets [13]. So the plate-like talc can be delaminated at relatively low external forces (such as shearing force), which accounts for the slippery feel of talc.

In the present work, we first attempted to use *in situ* polymerization of polar monomer to treat talc. Then, the modified talc was compounded with polypropylene in the molten state. By means of shearing forces during blending polypropylene with talc in a twin-screw extruder, the modified talc could be broken down into smaller stacks and even nanoscale sheets, producing nano-sized talc/polypropylene composites.

2. Experimental work

2.1. Materials

Talc powders (2500 mesh) were purchased from Sichuan Serpentine Mineral Factory in China. Methyl methacrylate (MMA) and butyl acrylate (BA) from Shanghai Chemical Co. (China) were purified by distillation under reduced pressure before use to remove the inhibitor. All of the water used was deionized. Isotactic polypropylene (PP) with a melt flow rate of 4 g/10 min under a trade name of Grade T30S was supplied by Wuhan Petrochemical Co. (China).

2.2. Modification of talc by in situ polymerization

Since poly(methyl methacrylate) (PMMA) and poly(butyl acrylate) (PBA) are partially compatible with PP, and their polar groups have dipole–dipole interaction with talc, MMA and BA were chosen to modify talc *via in situ* seed emulsion polymerization at 70 °C, respectively [20,21]. The experimental details are as follows: the weight ratio of monomer to talc was designed as 1:4, 1:2, and 1:1. Firstly, talc was dispersed ultrasonically in water. The ingredients (deionized water, sodium dodecyl sulfonate (SDS) as emulsifier, MMA or BA as monomer) were added to a 5000 ml glass reactor, heated and stirred continuously at 200 rpm, until the reaction temperature was reached. Then, an aqueous solution of ammonium persulfate (APS) with an amount of 1 wt% monomer was added to start the polymerization reaction. Before adding the initiator, the glass reactor equipped with stirrer was purged with N_2 six times. The products were spray-dried at 80 °C after emulsion breakage. Subsequently, they were dried at 60 °C under vacuum to a constant weight for about 48 h. The conversion of monomer was determined according to [20]. The last conversions of MMA and BA approached 97%–98% and 96%–97%, respectively. The modified talc was extracted with acetone for 24 h in a Soxhlet apparatus. The received solution was poured into methanol to obtain the extracted PMMA or PBA. The molecular mass and distribution of PMMA or PBA were characterized by Gel Permeation Chromatography (GPC, Aligent 1100 HPLC, America) equipped with the 79911GP-MXC column and RI detector at 25 °C in tetrahydrofuran solution at an elution rate of 1.0 ml/min against polystyrene standards. The number average molecular mass, weight average molecular mass and polydispersity index of PMMA were determined to be $\sim 3.54 \times 10^5$ g/mol, $\sim 5.72 \times 10^5$ g/mol and 1.62, respectively, while those of PBA were $\sim 1.43 \times 10^5$ g/mol, $\sim 9.26 \times 10^5$ g/mol and 6.45, respectively.

2.3. Preparation of talc/PP composites

The talc/PP composites were prepared by using a Werner & Pfleiderer ZSK-30 twin-screw extruder at barrel temperatures of 180–200 °C and a screw rotation speed of 300 rpm. The talc contents in all the composites were kept at 5 wt%. The extrudates were injection molded into rectangular bars (127 mm length, 12.7 mm width, and 6 mm thickness) in a BOY 22s dipronic injection molding machine with a barrel temperature of 200 °C and a mould temperature 60 °C for morphological and thermal properties characterization.

2.4. X-ray diffraction (XRD)

A Siemens D5000 X-ray diffractometer with Cu Kα radiation ($\lambda = 1.5406$ Å) at a generator voltage of 40 kV and a current of 30 mA was used to measure the diffraction behavior of talc and PP/talc composites. Measurements were conducted in the reflection mode at ambient temperature with a scanning speed of 1°/min and a step size of 0.01°. 2θ varied from 1° to 15° and 6° to 40° for pristine and modified talc, and from 1° to 8° and 10° to 35° for PP/talc composites.

2.5. Scanning electron microscope (SEM)

The morphologies of talc, modified talc by *in situ* seed emulsion polymerization of MMA or BA, and the fracture surfaces of composites were observed with a Philips XL30 scanning electron microscope (SEM). All fracture surfaces were coated with a thin layer of gold before examination by SEM.

2.6. Transmission electron microscopy (TEM)

The specimens of talc/PP composites for TEM were ultramicrotomed to 60 nm thick sections with a diamond knife in a liquid nitrogen environment using a Reichert-Jung Ultracut E

microtome. Sections were collected on 300 mesh copper TEM grids, dried with filter paper and examined by a Philips CM12 TEM at an accelerating voltage of 120 kV.

2.7. Differential scanning calorimetry (DSC)

DSC measurements were conducted using a TA 2910 DSC instrument at a heating rate of 10 °C/min under dry nitrogen atmosphere. Before DSC recording, all samples were heated to 200 °C and kept at this temperature for 3 min before being quenched to ambient temperature to eliminate the influence of any previous thermal histories. For nonisothermal crystallization measurements, samples were heated to 200 °C at a rate of 10 °C/min, kept at 200 °C for 3 min, and then cooled to 30 °C at a rate of 10 °C/min.

2.8. Dynamic mechanical analysis (DMA)

DMA was conducted with a TA instruments dynamic mechanical analyzer (Model 2980 TA Instruments, Newcastle, DE). The dynamic temperature spectra of the samples with a dimension of $25 \times 12 \times 4$ mm^3 were obtained in single cantilever mode at a fixed vibration frequency of 1 Hz and oscillation amplitude of 0.03 mm. The temperature range studied was from −60 to 120 °C with a heating rate of 3 °C/min.

3. Results and discussion

3.1. Microstructures

Fig. 1 shows small and wide-angle XRD patterns of pristine talc and PMMA-modified talc. It can be seen that pristine talc has a characteristic peak (designated as Peak I) at $2\theta = 6.31°$, corresponding to a basal spacing of 1.4 nm. The peak position does shift after talc is modified by *in situ* polymerization of MMA. It indicates that PMMA formed during *in situ* polymerization does not intercalate into the intra-galleries of talc.

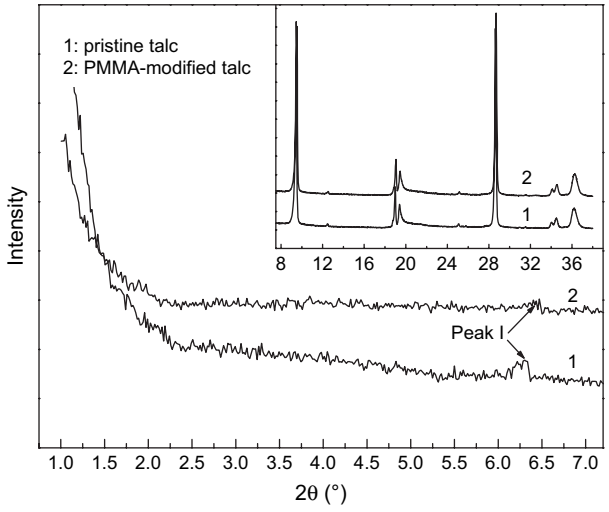

Fig. 1. XRD patterns of pristine and PMMA-modified talc ($W_{PMMA}/W_{talc} = 1{:}4$).

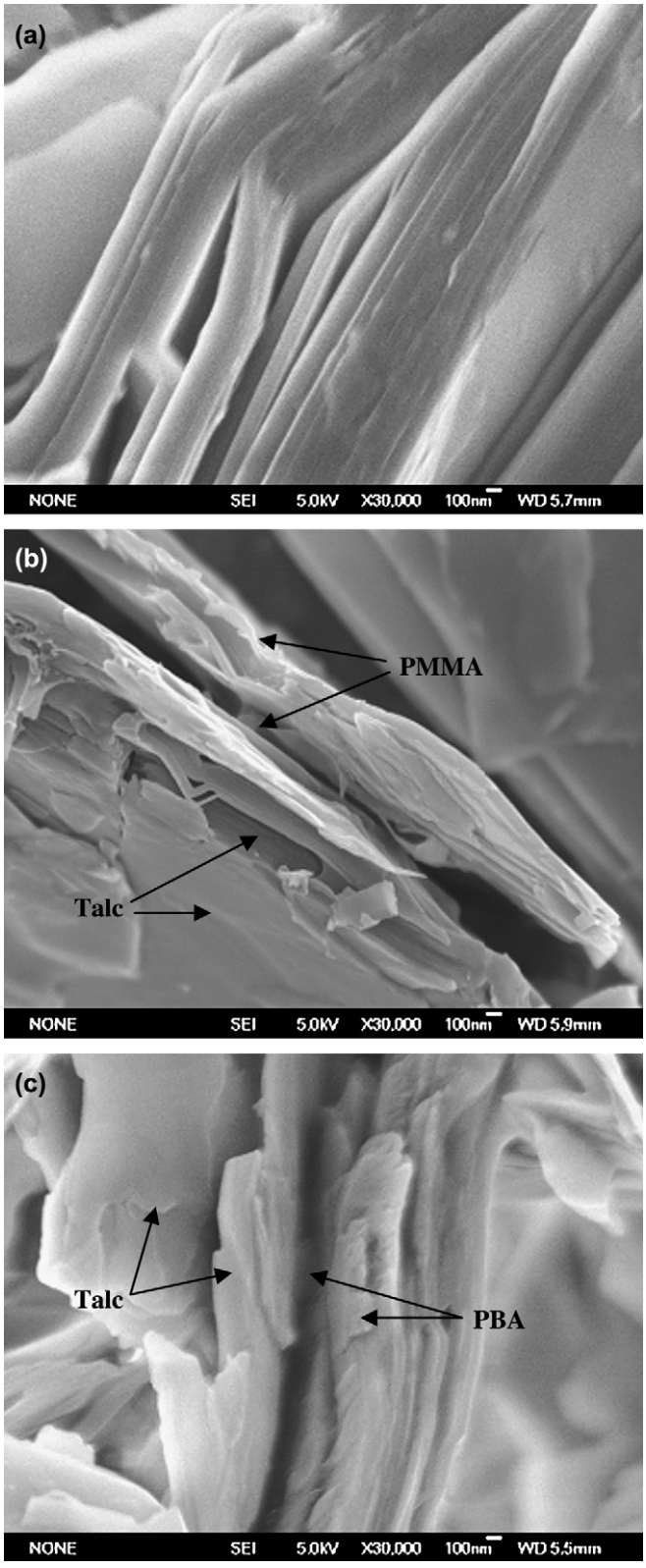

Fig. 2. SEM micrographs of pristine and modified talc fillers: (a) pristine talc, (b) PMMA-modified talc ($W_{PMMA}/W_{talc} = 1{:}4$), (c) PBA-modified talc ($W_{PBA}/W_{talc} = 1{:}4$).

Moreover, *in situ* polymerization does not affect the crystal structure of talc at wide-angle region (see the inset of Fig. 1). Fig. 2 shows SEM micrographs of pristine and modified talc.

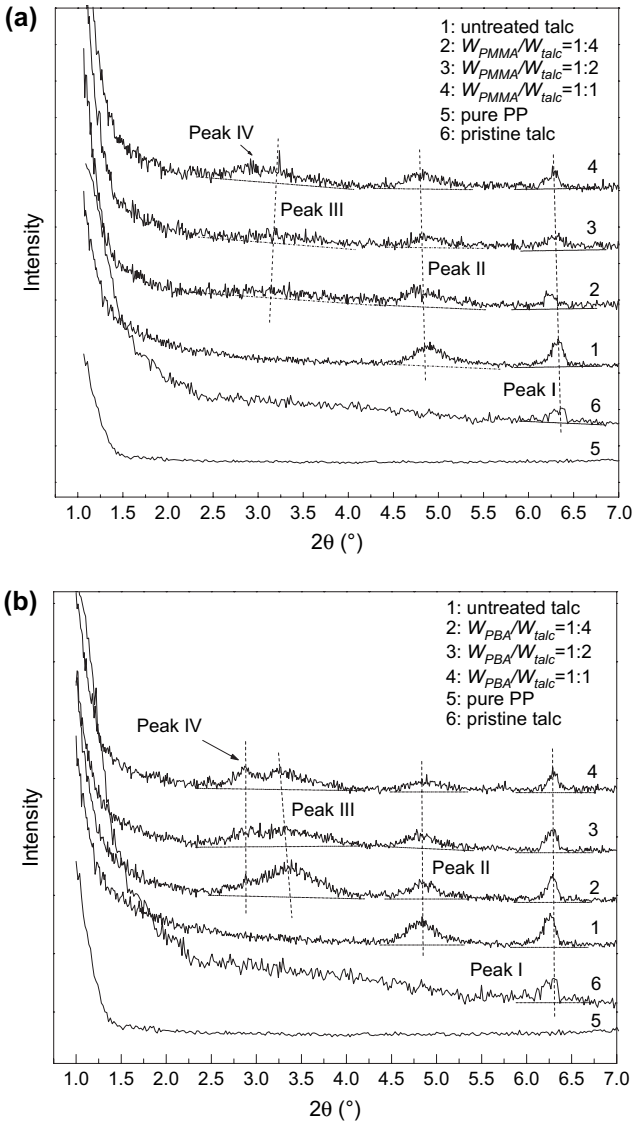

Fig. 3. XRD patterns of talc/PP composites: (a) PMMA-modified talc and (b) PBA-modified talc.

The layered structure of pristine talc is clear. After it was modified by *in situ* polymerization, its surface and interlayer gaps became blurry. It also proves that PMMA or PBA macromolecules cover the surface of talc layers during *in situ* polymerization.

Fig. 3 shows the small-angle XRD patterns of talc/PP composites. Compared with pristine talc, a new characteristic peak (designated as Peak II) for the untreated talc/PP composite appears at $2\theta = 4.86°$, corresponding to a basal spacing of 1.8 nm. And there is no characteristic peak in XRD curve of pure PP. It implies that PP macromolecules intercalate into the galleries of the partial talc layers under heating and shearing forces when talc is blended with PP during melt compounding. Furthermore, after talc is modified by *in situ* polymerization of MMA, a third diffraction peak (designated as Peak III) appears at $2\theta = 3.28°$ ($d = 2.7$ nm). With increasing weight ratio of PMMA and talc (W_{PMMA}/W_{talc}), the diffraction intensity ratio of Peak III and Peak II increases.

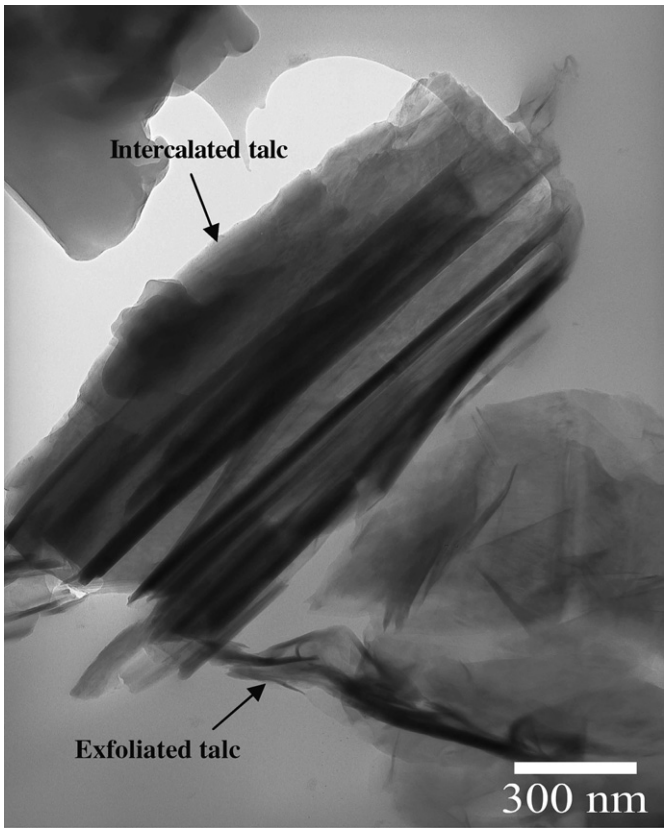

Fig. 4. TEM micrograph of PBA-modified talc/PP composite ($W_{PBA}/W_{talc} = 1:4$).

Interestingly, when W_{PMMA}/W_{talc} is up to 1:1, the fourth peak (designated as Peak IV) appears at $2\theta = 3.05°$ ($d = 2.8$ nm). Similarly, in the PBA-modified talc/PP composites, peak III appears at $2\theta = 3.36°$ ($d = 2.6$ nm). With increasing weight ratio of BA and talc (W_{PBA}/W_{talc}), peak III shifts to $2\theta = 3.28°$ ($d = 2.7$ nm), and the diffraction intensity ratio of peak III and peak II also increases (Fig. 3(b)). It is worthwhile to note that a fourth peak (peak IV) at $2\theta = 2.87°$ ($d = 3.1$ nm) appears when W_{PBA}/W_{talc} is only 1:4 and its intensity increases with the ratio of W_{PBA}/W_{talc}.

Fig. 4 shows TEM micrograph of PBA-modified talc/PP composite ($W_{PBA}/W_{talc} = 1:4$). It is clear that talc layers are intercalated. Also, some exfoliated talc layers are observed in PP matrix. Figs. 5–7 are SEM micrographs of freeze-fractured surfaces of PP composites with untreated and modified talcs. It can be seen that the talc layers are aligned along the injection flow direction, and uniformly dispersed in the PP matrix. For the untreated talc/PP composite, talc is dispersed in PP with an average thickness ~2.2 μm (Fig. 5(a)), and the interfacial adhesion between talc and PP seems poor (Fig. 5(b)). Due to shearing during melt compounding, some talc layers are delaminated to 280–670 nm in thickness (Fig. 5(b)). However, for PMMA-modified talc, most layers are delaminated to 80–240 nm in thickness (Fig. 6(b)). Moreover, for PBA-modified talc/PP composites, the PBA-modified talc layers in composites are thinner, and the interfacial adhesion between PBA-modified talc layer and PP appears better than

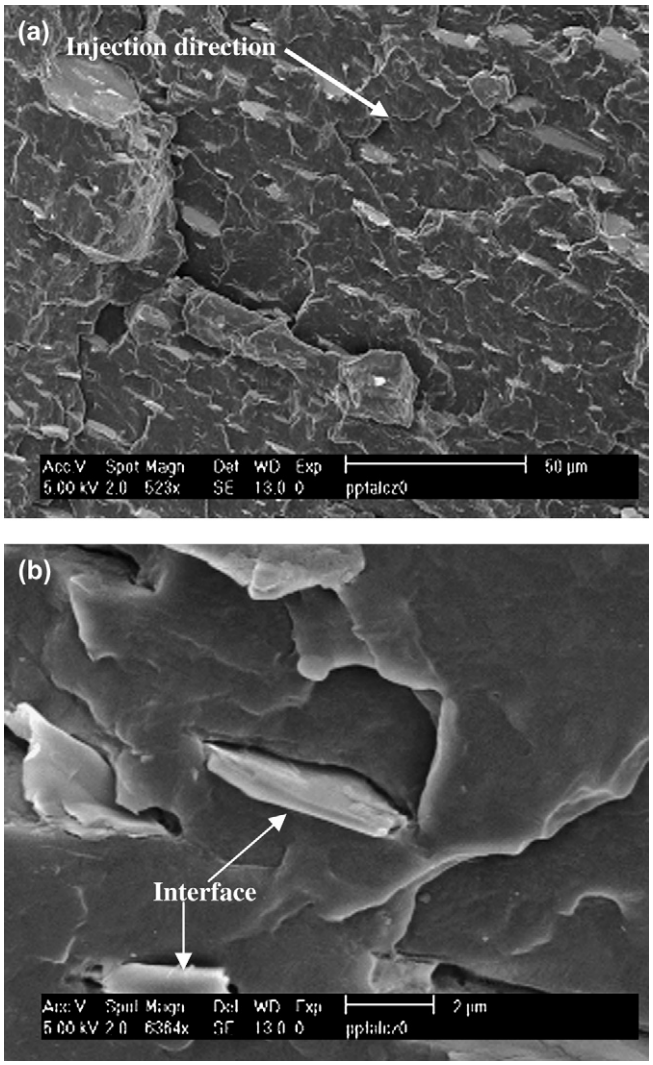

Fig. 5. SEM micrographs of cryo-fractured surface of untreated talc/PP composite at (a) low and (b) high magnifications.

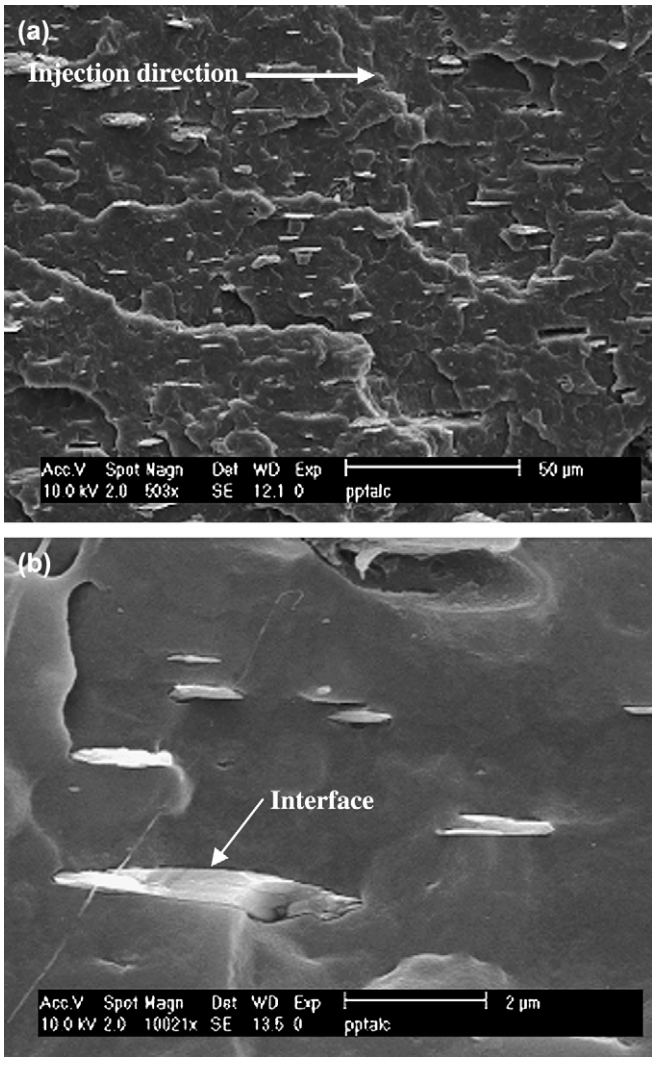

Fig. 6. SEM micrographs of cryo-fractured surface of PMMA-modified talc/PP composite ($W_{PMMA}/W_{talc} = 1{:}4$) at (a) low and (b) high magnifications.

that between PP and PMMA-modified talc (Fig. 7(b)). The above results can be understood from the view of the structure of talc and their compatibility. It is well-known that there is no layer charge in the galleries of talc, but the weak interlayer interaction leads to easy slip of its stacking layers under shearing forces, the galleries of the partial talc layers are enlarged by PP during melt compounding. Thereby, there exists a wide distribution of the basal spacing of the intra-galleries of talc in the composite. Additionally, based on theoretical calculation [22], the solubility parameters of PP, PMMA and PBA are 17.0, 19.0 and 18.3 $(J\,cm^{-3})^{1/2}$, respectively. PMMA and PBA are not miscible with PP, the interaction between PMMA and PP, especially between PBA and PP is stronger than that between PP and talc. In addition, there is a dipole–dipole interaction between talc and polar PMMA and PBA macromolecules covering the talc layers. These two factors benefit the diffusion of PP macromolecules into the intra-galleries of talc during melt compounding. Thus the PBA formed during *in situ* polymerization is more helpful for the PP macromolecular chains to diffuse into the intra-galleries of talc during subsequent melt compounding, and to enhance the interface adhesion between PP and talc layers. These characteristics improve the performance of polymer composites.

3.2. Thermal properties

The DSC thermograms of modified talc/PP composites are shown in Figs. 8 and 9. Their onset melting temperature (T_m), peak melting temperature (T_{mp}), melting range (T_R, defined as the temperature difference between initial and terminal points of melting) under heating scan, and crystallization temperature (T_c, determined as the temperature at the intercept of the tangents at the high temperature side of the exotherm and the baseline), initial temperature of crystallization (T_0) and peak crystallization temperature (T_{cp}) under cooling scan are listed in Table 1. Compared with untreated talc/PP composites, the crystallization temperatures of the PP phase in the composites, such as T_c, T_0 and T_{cp}, tend to increase after the talc is modified by *in situ* polymerization of MMA with W_{PMMA}/W_{talc}

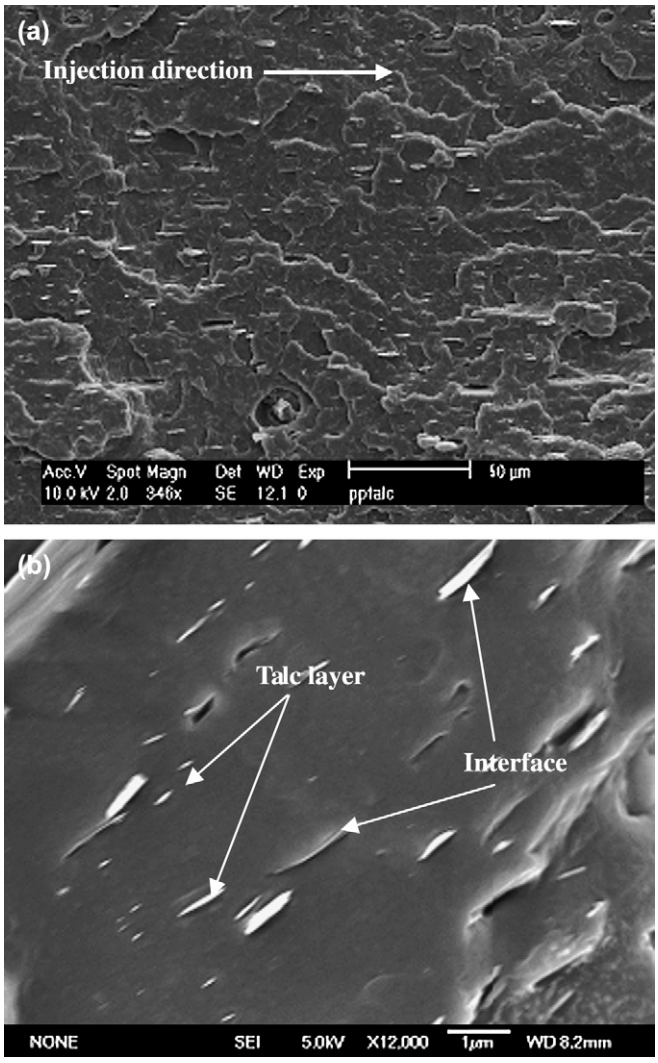

Fig. 7. SEM micrographs of cryo-fractured surface of PBA-modified talc/PP composite ($W_{PBA}/W_{talc} = 1{:}4$) at (a) low and (b) high magnifications.

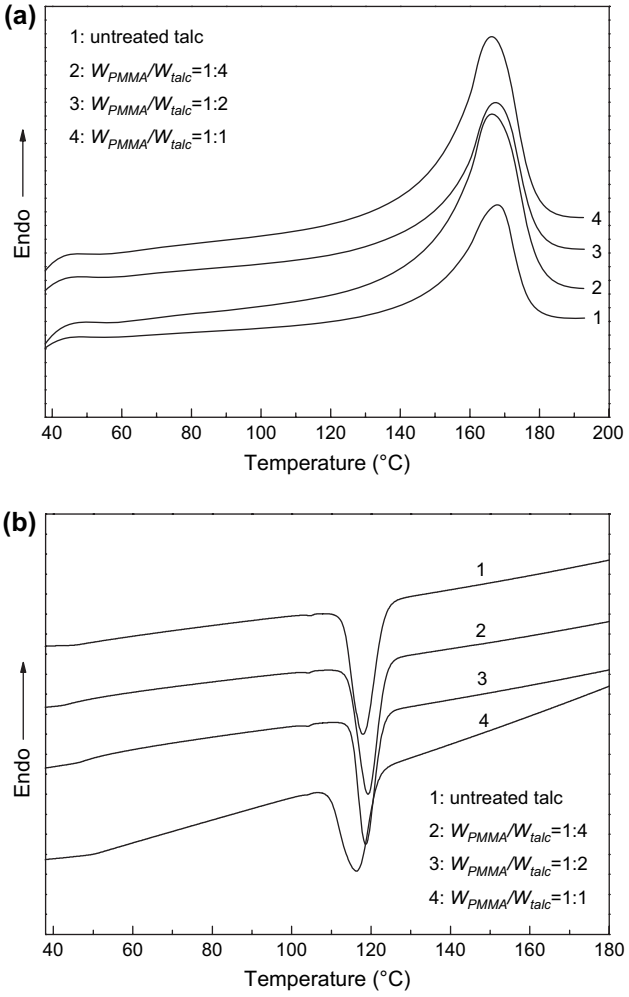

Fig. 8. DSC curves of PMMA-modified talc/PP composites under (a) heating and (b) cooling scans.

ratio of 1:4. In general, talc acts as a nucleating agent to induce crystallization of polypropylene [23,24]. And the *in situ* polymerization of MMA improves the dispersion of talc in PP matrix, leading to an enhanced nucleation rate of PP crystallization in composites. It should be noted that with increasing W_{PMMA}/W_{talc} ratio, the above crystallization temperatures of PP phase in composites tend to decrease. For PBA-modified talc/PP composites, these temperatures decrease with increasing weight ratio of PBA to talc more obviously, which implies that the nucleation rate of crystallization slows down after PBA or PMMA macromolecules attached on the surface of talc layers. On the other hand, as Gupta and Purwar reported, the parameter ($\Delta T = T_c - T_{cp}$) can be used to characterize the crystallization growth rate of PP melts [25]. The decrease in ΔT indicates that the crystallization of the polymer is accelerated. From the ΔT values in Table 1, the crystallization rate of the PP phase in modified talc/PP composites is slightly higher than that of untreated talc/PP composite due to the improved dispersion of talc in PP matrix. However, the ΔT values tend to increase with the ratio of W_{PMMA}/W_{talc} or W_{PBA}/W_{talc}, which implies that *in situ* polymerization modification weakens the nucleation effect of talc on crystallization of PP indeed.

For nonisothermal crystallization process of polymer, the relative crystallinity $X(T)$, which is a function of crystallization temperature, can be obtained from [26–29]:

$$X(T) = \frac{\int_{T_0}^{T} (dH_c/dT)dT}{\int_{T_0}^{T_\infty} (dH_c/dT)dT} = \frac{\int_{T_0}^{T} (dH_c/dT)dT}{\Delta H_c} \quad (1)$$

where T_0, T and T_∞ are the initial crystallization temperature, the crystallization temperature at arbitrary time and after the completion of the crystallization process, respectively. dH_c denotes the measured enthalpy for crystallization during an infinitesimal temperature interval dT while ΔH_c represents the total enthalpy of crystallization.

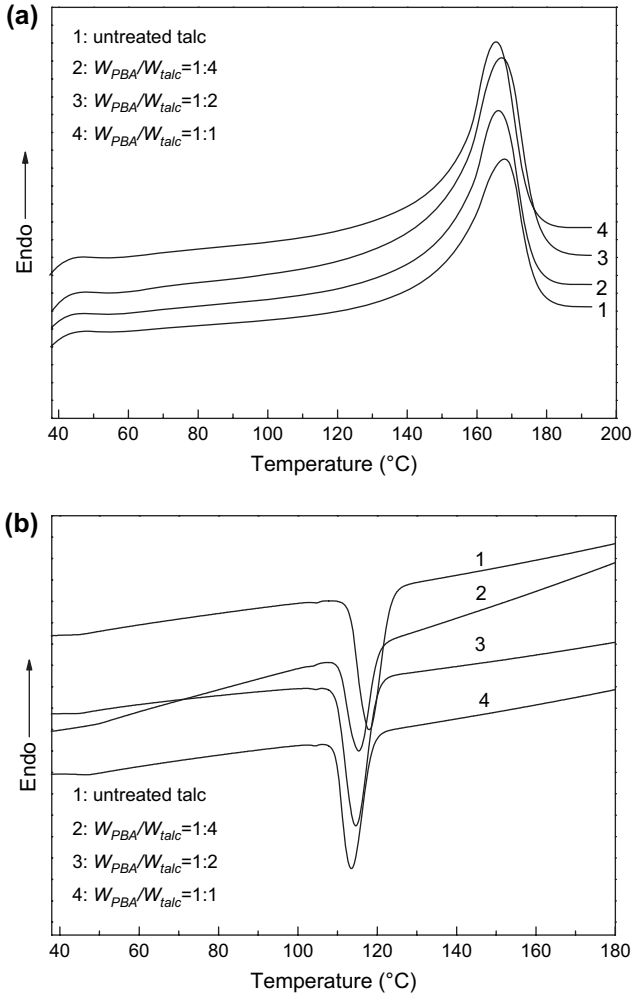

Fig. 9. DSC curves of PBA-modified talc/PP composites under (a) heating and (b) cooling scans.

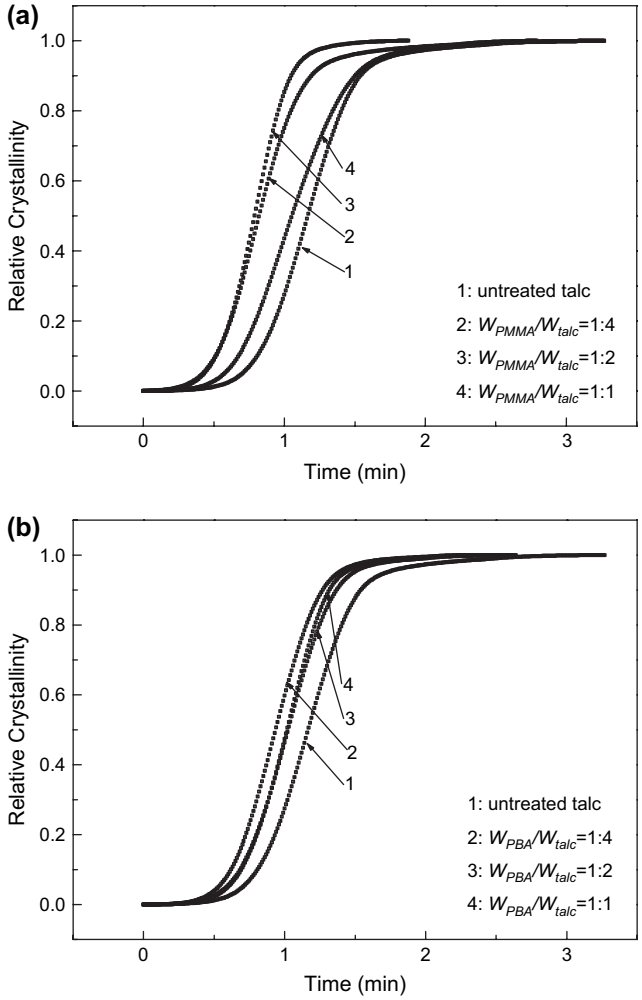

Fig. 10. Plot of relative crystallinity vs. crystallization time for nonisothermal crystallization of (a) PMMA-modified talc/PP composites and (b) PBA-modified talc/PP composites.

The crystallization temperature T can be converted to crystallization time t by [28]:

$$t = \frac{|T_0 - T|}{\phi} \tag{2}$$

where φ is the cooling rate and is 10 °C/min here.

Based on Eq. (1) and DSC curves in Figs. 8 and 9, the relationship of relative crystallinity $X(T)$ against temperature (T) is obtained. Accordingly, the relative crystallinity as a function of time $X(t)$ can be transferred from $X(T)$ curves *via* Eq. (2), which is shown in Fig. 10. The received half crystallization time ($t_{1/2}$) values are also listed in Table 1. It can be seen that the $t_{1/2}$ value of PP phase in modified talc/PP composite is smaller than that in untreated talc/PP composite, and increases with the ratio of W_{PMMA}/W_{talc} or W_{PBA}/W_{talc}. This result is consistent with that derived from the crystallization temperature and ΔT values above.

The degree of crystallinity (X_c) of the modified talc/PP composites is determined based on their melting heat normalized to that of PP according to:

Table 1
Melting and crystallization properties of PP phase in modified talc/PP composites

Sample	T_m (°C)	T_{mp} (°C)	T_c (°C)	T_0 (°C)	T_{cp} (°C)	ΔT[a] (°C)	T_R (°C)	$t_{1/2}$ (min)	X_c (%)
Untreated talc	150.9	168.4	122.6	126.6	117.9	4.7	90.0	1.16	40.6
W_{PMMA}/W_{talc} = 1:4	153.0	166.3	123.4	127.2	119.3	4.1	90.8	0.82	37.4
W_{PMMA}/W_{talc} = 1:2	153.5	167.4	123.0	126.4	118.6	4.4	89.2	0.80	38.7
W_{PMMA}/W_{talc} = 1:1	152.6	166.3	121.1	124.6	116.4	4.7	89.0	1.06	38.0
W_{PBA}/W_{talc} = 1:4	152.8	166.2	119.5	123.7	115.4	4.1	88.0	0.94	38.6
W_{PBA}/W_{talc} = 1:2	152.6	167.2	119.0	122.8	114.5	4.5	88.0	1.02	34.3
W_{PBA}/W_{talc} = 1:1	153.6	165.5	117.9	122.2	113.5	4.4	85.6	1.02	33.1

[a] $\Delta T = T_c - T_{cp}$.

$$X_c = \frac{\Delta H_m}{\Delta H^*} \times 100\% \quad (3)$$

where ΔH_m is the melting heat of the modified talc/PP composite normalized to that of PP and ΔH^* is the melting heat of PP with 100% crystallinity. From [22], the value of ΔH^* for 100% crystalline PP is 8.7 kJ/mol. Table 1 shows that the crystallinity of the modified talc/PP composites is lower than that of untreated talc/PP composite. While this decreases with increasing ratio of W_{PBA}/W_{talc}, the trend is not as obvious with W_{PMMA}/W_{talc}. As discussed above, during *in situ* MMA/talc or BA/talc polymerization, the PMMA or PBA macromolecules cover the surface of the talc layers and enhance the interaction between PP and talc. Hence, it hinders the crystallization capability of PP in terms of crystallinity compared to the untreated talc/PP composites. This result is consistent with those of compatibilized polymer composites [30].

In addition, the modified talc elevates T_m of PP crystal phase in the composites. Hence, the improved dispersion of talc in PP matrix increases the crystalline lamellar thickness l_c according to the following Thomson–Gibbs equation [31]:

$$T_m = T_{m0}\left(1 - \frac{2\sigma_e}{l_c \Delta H_{100}}\right) \quad (4)$$

where T_{m0} is the melting point for a hypothetical crystal of infinite size; σ_e is the fold surface energy which is related to the surface energy of the crystal end faces where the chains fold. Compared to the talc modified with *in situ* polymerization, pristine talc is not dispersed uniformly in PP matrix, which would result in wider size distribution (melting range T_R widening, shown in Table 1) and more defects of the crystallites. Both factors lead to reductions in the T_m of PP phase in the talc/PP composites.

Further, the T_m values of PP phase in PMMA-modified talc/PP and PBA-modified talc/PP composites are very similar. Compared to the PMMA-modified talc/PP composites, the PBA-modified talc/PP composites, at the same weight ratio of polymer to talc, have lower crystallization temperature and crystallinity. These results should be attributed to the better compatibility between PBA and PP than that between PMMA and PP.

3.3. Dynamic mechanical properties

Figs. 11 and 12 show DMA curves of the modified talc/PP composites. The storage moduli (E') of PMMA-modified talc/PP composites are higher than those of untreated talc/PP composites due to PMMA possessing a high modulus value when the weight ratio of PMMA and talc is 1:4. Nevertheless, storage moduli of PMMA-modified talc/PP composites tend to decrease with increasing W_{PMMA}/W_{talc}. On the other hand, the E' values of PMMA-modified talc/PP composites are higher than those of PBA-modified talc/PP composites because of the higher flexibility of PBA, even though the incorporation of PBA in talc/PP composites is small (1.25–5 wt%). In contrast,

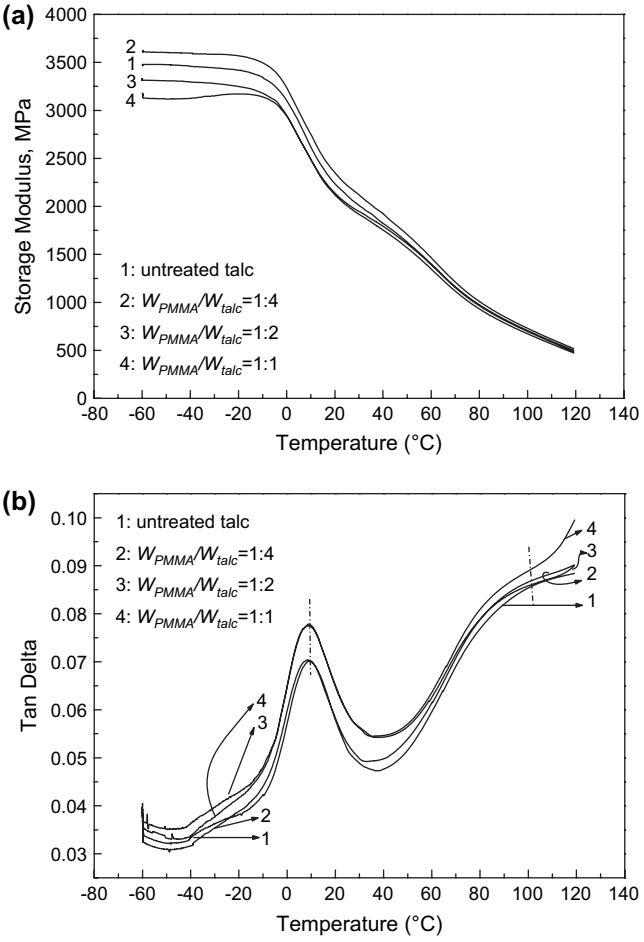

Fig. 11. DMA curves of PMMA-modified talc/PP composites: (a) storage modulus (E') and (b) tan δ.

there are two transitions in PBA-modified talc/PP composites, which are related to the glass transition (T_{g1}, at about 9 °C) of PP and that (T_{g2}, at about −30–−35 °C) of PBA chains. For PMMA-modified talc/PP composites, the glass transition (T_{g2}) of PMMA chains is not obvious. Only when the ratio $W_{PMMA}/W_{talc,}$ is up to 1:2, the glass transition of PMMA appears at about 100 °C, which is close to the value of 104 °C given in [22]. These results indicate that PP is not thermodynamically miscible with PMMA or PBA. The glass transition temperatures of the modified talc/PP composites are listed in Table 2. The T_{g1} values of PP phase in different modified talc/PP composites are independent of the ratio W_{PMMA}/W_{talc} or W_{PBA}/W_{talc}. Increasing the ratio of W_{PMMA}/W_{talc} or W_{PBA}/W_{talc} only leads to increasing values of loss factor (tan δ) of related talc/PP composites.

3.4. Crystal structures

Generally, the crystal structure of a polymer matrix can be significantly affected by the addition of inorganic filler. The alignment of fillers will induce orientation of the polymer crystals during the injection molding process [32]. Fig. 13 shows the WAXD curves of PP and its composites. Neat PP

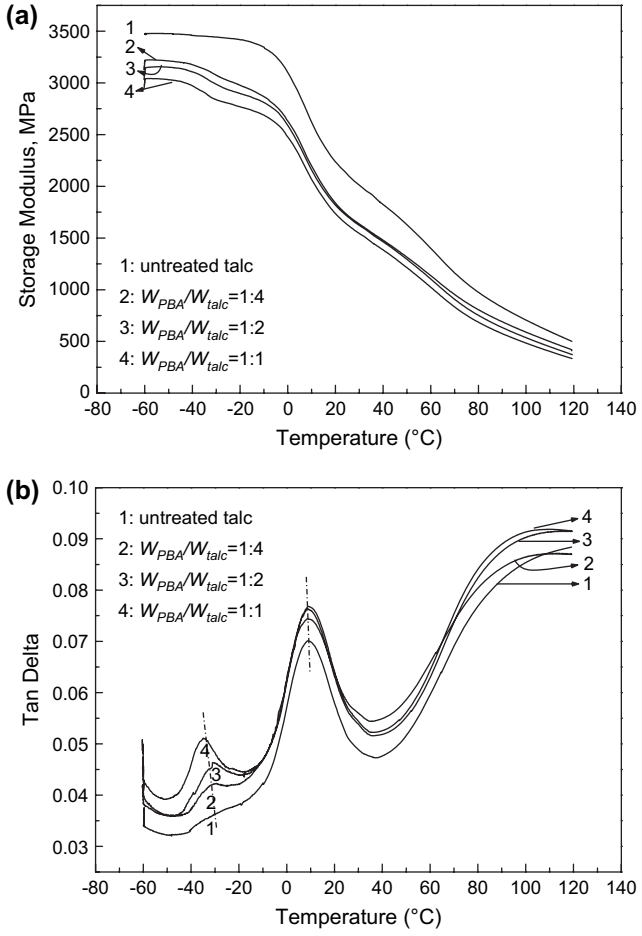

Fig. 12. DMA curves of PBA-modified talc/PP composites: (a) storage modulus (E') and (b) tan δ.

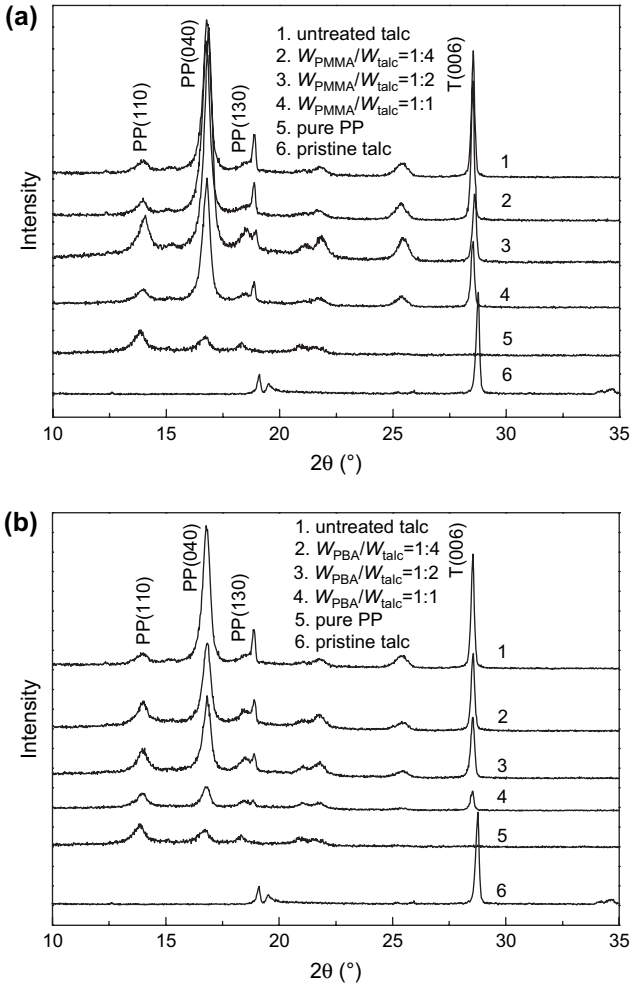

Fig. 13. WAXD curves of neat PP and talc/PP composites: (a) PMMA-modified talc and (b) PBA-modified talc.

shows strong diffraction peaks at 13.86°, 16.84° and 18.35°, respectively, corresponding to the (110), (040) and (130) diffraction planes of α-PP crystals with a monoclinic configuration [31,33]. The inter-planar spacing (d) values for the various peaks are calculated by Bragg's equation. The d values and relative reflection intensities of different diffraction planes are listed in Table 3. The (110) plane of neat PP has the strongest relative reflection intensity. The incorporation of untreated talc and modified talc has little influence on the inter-planar spacing d values of (110), (040) and (130) planes, but decreases sharply the relative reflection intensities of (110) and (130) planes, and noticeably increases the intensity of (040) plane. Since the talc layers in the talc/PP composites are aligned along the flow direction during injection molding, this could also induce a preferential orientation of the PP macromolecular chains. As reported in [32,34], PP crystals grow along their b-axes perpendicular to the planes of talc layers in talc-filled PP system, and the ratio ($I_{(040)}/I_{(110)}$) of the reflection intensities of the (040) and (110) planes could be used to characterize the degree of the b-axis orientation. As shown in Table 3, the $I_{(040)}/I_{(110)}$ value of neat PP is 0.78, indicating that the distribution of the PP crystal is approximately isotropic. However, the $I_{(040)}/I_{(110)}$ value of the untreated talc/PP composite increases to 7.52. It is believed that the peculiar orientation of PP crystal in untreated talc/PP composite originates from the flaky shape and crystallization nucleation of talc. It should be noted that the $I_{(040)}/I_{(110)}$ values of the modified talc/PP composites decrease with increasing ratio of W_{PMMA}/W_{talc} or W_{PBA}/W_{talc}, especially in the case of PBA-modified talc. For example, when W_{PBA}/W_{talc} ratio is 1:1, the $I_{(040)}/I_{(110)}$ value of PBA-modified talc/PP composite changes to 1.34 from 7.52 of untreated talc/PP composite. This indicates that the degree of PP crystal orientation decreases because the orientation effect and crystallization

Table 2
Dynamic mechanical properties of modified talc/PP composites

Sample	T_{g1} (°C)	Tan δ at T_{g1} ($\times 10^{-2}$)	T_{g2} (°C)	Tan δ at T_{g2} ($\times 10^{-2}$)
Untreated talc	8.9	7.01	–	–
W_{PMMA}/W_{talc} = 1:4	8.5	7.04	–	–
W_{PMMA}/W_{talc} = 1:2	9.2	7.79	~100	8.58
W_{PMMA}/W_{talc} = 1:1	8.9	7.75	~100	8.88
W_{PBA}/W_{talc} = 1:4	8.7	7.44	−30.8	4.20
W_{PBA}/W_{talc} = 1:2	8.7	7.64	−31.1	4.63
W_{PBA}/W_{talc} = 1:1	9.1	7.68	−34.9	5.11

Table 3
XRD data for PP and different talc/PP composites

	Diffraction peak	2θ (°)	d (Å)	I (%)	$I_{(040)}/I_{(110)}$
Pure PP	$(110)_\alpha$	13.86	6.38	100	
	$(040)_\alpha$	16.84	5.29	77.9	0.78
	$(130)_\alpha$	18.35	4.83	54.6	
Untreated talc	$(110)_\alpha$	13.96	6.34	13.3	
	$(040)_\alpha$	16.81	5.27	100	7.52
	$(130)_\alpha$	18.88	4.70	27.9	
$W_{PMMA}/W_{talc} = 1{:}4$	$(110)_\alpha$	13.96	6.34	13.3	
	$(040)_\alpha$	16.87	5.28	100	7.52
	$(130)_\alpha$	18.87	4.70	21.9	
$W_{PMMA}/W_{talc} = 1{:}2$	$(110)_\alpha$	14.06	6.30	21.2	
	$(040)_\alpha$	16.87	5.253	100	4.72
	$(130)_\alpha$	18.93	4.69	14.1	
$W_{PMMA}/W_{talc} = 1{:}1$	$(110)_\alpha$	14.00	6.33	15.5	
	$(040)_\alpha$	16.79	5.27	100	6.45
	$(130)_\alpha$	18.85	4.70	20.9	
$W_{PBA}/W_{talc} = 1{:}4$	$(110)_\alpha$	13.98	6.33	35.3	
	$(040)_\alpha$	16.82	5.27	100	2.82
	$(130)_\alpha$	18.89	4.70	37.0	
$W_{PBA}/W_{talc} = 1{:}2$	$(110)_\alpha$	14.01	6.33	37.4	
	$(040)_\alpha$	16.83	5.26	100	2.67
	$(130)_\alpha$	18.89	4.69	31.3	
$W_{PBA}/W_{talc} = 1{:}1$	$(110)_\alpha$	14.01	6.33	74.5	
	$(040)_\alpha$	16.79	5.28	100	1.34
	$(130)_\alpha$	18.85	4.70	48.2	

nucleation of talc on PP crystals are hindered by the presence of PMMA or PBA on the surface of talc. These observations are consistent with the DSC results.

4. Conclusions

The talc/PP nanocomposites with nano-sized intercalated structure are formed by compounding PP with talc modified by *in situ* polymerization of MMA or BA. The delaminated talc layers are aligned along the flow direction and dispersed in PP matrix more uniformly. When talc is modified by *in situ* polymerization of MMA, the thickness of delaminated layers varies from 80 nm to 240 nm. Since there is better compatibility between PBA and PP, the talc layers in PBA-modified talc/PP composites are delaminated into thinner layers. The PMMA or PBA macromolecule formed covers the surface of the talc layers enhancing the interaction between PP and talc, thereby hindering the crystallization of PP in terms of crystallization nucleation and crystallinity. The flow-aligned talc layers also induce the orientation of PP crystals. But this orientation is decreased with addition of PMMA and PBA.

Acknowledgments

This work was funded by the National Natural Science Foundation of China (Grant No. 50573026), Foundation of State Key Laboratory of Plastic Forming Simulation and Die & Mould Technology, China, Program for New Century Excellent Talents in University of China and the Australian Research Council (ARC). Y.-W. Mai wishes to acknowledge the award of an Australian Federation Fellowship tenable at the University of Sydney. Support of an Australian Postdoctoral Fellowship to Z.-Z. Yu by the ARC is also very much appreciated.

References

[1] Yano K, Usuki A, Okada A, Kurauchi T, Kamigaito O. J Polym Sci Part A Polym Chem 1993;31(10):2493–8.
[2] Okamoto M, Morita S, Taguchi H, Kim YH, Kotaka T, Tateyama H. Polymer 2000;41(10):3887–90.
[3] Baughman RH, Zakhidov AA, De Heer WA. Science 2002;297(5582):787–92.
[4] Xie XL, Mai Y-W, Zhou XP. Mater Sci Eng R 2005;49(4):89–112.
[5] Gilman JW, Jackson CL, Morgan AB, Harris R, Manias E, Giannelis EP, et al. Chem Mater 2000;12(7):1866–73.
[6] Cho JW, Paul DR. Polymer 2001;42(3):1083–94.
[7] Bhiwankar NN, Weiss RA. Polymer 2005;46(18):7246–54.
[8] Dasari A, Yu ZZ, Mai Y-W. Polymer 2005;46(16):5986–91.
[9] Ray SS, Okamato M. Prog Polym Sci 2003;28(11):1539–641.
[10] Alexandre M, Dubois P. Mater Sci Eng R 2000;28(1–2):1–63.
[11] Zanetti M, Lomakin SG, Camino G. Macromol Mater Eng 2000;279(1):1–9.
[12] Nam PH, Kaneko M, Ninomiya N, Fujimori A, Masuko T. Polymer 2005;46(18):7403–9.
[13] Zbik M, Smart RStC. Miner Eng 2002;15(4):277–86.
[14] Radosta JA, Trivedi NC. In: Katz HS, Milewski JV, editors. Handbook of fillers and reinforcements for plastics. New York: Van Nostrand Reinhold Co; 1978. p. 160–70.
[15] Wu G, Wen B, Hou S. Polym Int 2004;53(6):49–55.
[16] Denac M, Musil V, Šmit I. Composites Part A 2005;36(9):1282–90.
[17] Garcia-Martinez JM, Laguna O, Collar EP. J Polym Eng 1997;17(4):269–80.
[18] Taranco J, Garcia-Martinez JM, Laguna O, Collar EP. J Polym Eng 1994;13(4):287–304.
[19] Sánchez-Soto PJ, Wiewióra A, Avilés MA, Justo A, Pérez-Maqueda LA, Pérez-Rodríguez JL, et al. Appl Clay Sci 1997;12(4):297–312.
[20] Xie XL, Li BG, Pan ZR, Li RKY, Tjong SC. J Appl Polym Sci 2001;80(11):2105–12.
[21] Xie XL, Li RKY, Liu QX, Mai Y-W. Polymer 2004;45(8):2793–802.
[22] Van Krevelen DW. Properties of polymer. 3rd ed. New York: Elsevier Science; 1990. p. 120–202.
[23] Ferrage E, Martin F, Boudet A, Petit S, Fourty G, Jouffret F, et al. J Mater Sci 2002;37(8):1561–73.
[24] Naike M, Fuku Y, Matsumura T, Nomura T. J Appl Polym Sci 2001;79(9):1693–703.
[25] Gupta Ak, Purwar SN. J Appl Polym Sci 1984;29(5):1595–609.
[26] Papageorigiou GZ, Achilias DS, Bikiaris DN, Karayannidis GP. Thermochim Acta 2005;427(1–2):117–28.
[27] Liu SL, Chung TS. Polymer 2000;41(8):2781–93.
[28] Supaphol P, Thanomkiat P, Phillips RA. Polym Test 2004;23(8):881–95.
[29] Supaphol P. Thermochim Acta 2001;370(1–2):37–48.
[30] Xie XL, Fung KL, Li RKY, Tjong SC, Mai Y-W. J Polym Sci Part B Polym Phys 2002;40(12):1214–22.
[31] Hoffman JD, Davis Jr GT, Lauritzen JI. In: Hannay NB, editor. Treatise on solid state chemistry, vol. 3. New York: Plenum Press; 1976. p. 528.
[32] Alonso M, Velasco JI, De Saja JA. Eur Polym J 1997;33(3):255–62.
[33] Karger-Kocsis J. Polypropylene: structure, blends and composites. London: Chapman-Hall; 1995. p. 33.
[34] Fujiyama M, Wakino T. J Appl Polym Sci 1991;42(1):9–20.